THE STUDY OF THE USE OF TETHERS FOR PAYLOAD ORBITAL TRANSFER

CONTINUATION OF INVESTIGATION OF ELECTRODYNAMIC STABILIZATION AND CONTROL OF LONG ORBITING TETHERS

Contract NAS8-33691

Monthly Progress Report #19

For the period 1 November 1982 thru 31 December 1982

Principal Investigator

Dr. Giuseppe Colombo

January 1983

Smithsonian Institution
Astrophysical Observatory
Cambridge, Massachusetts 02138

THE STUDY OF THE USE OF TETHERS FOR PAYLOAD ORBITAL TRANSFER

CONTINUATION OF INVESTIGATION OF ELECTRODYNAMIC STABILIZATION AND CONTROL OF LONG ORBITING TETHERS

Contract NAS8-33691

Monthly Progress Report #19

For the period 1 November 1982 thru 31 December 1982

Principal Investigator
Dr. Giuseppe Colombo

Co-Investigators
Dr. Mario D. Grossi
Mr. David Arnold
Dr. Manuel Martinez-Sanchez

ACKNOWLEDGEMENT

The author of this report is

Mr. David Arnold

Table of Contents

1.0 Release of A Heavy Payload From the End of the Tether

1.1 Discussion of Approach

One of the potential uses of the tether is for launching a payload into a higher orbit by deploying it from the Shuttle or a space station on a long tether and then releasing it. The release would cause a sudden loss of force on the end of the wire resulting in recoil of the launching mechanism remaining at the end of the wire. Under a previous contract some initial analyses were done to study methods of avoiding recoil and loss of tension in the wire after payload release. A maneuver with the reel motor was stimulated which pulled the payload toward the Shuttle and released it while the wire was under a lower tension approximately equal to the equilibrium value for the remaining mass. The initial study of this technique is described in the report "Investigation of Electrodynamic Stabilization and Control of Long Orbiting Tethers," G. Colombo, March 1981. In that study the payload released was 10 tons and the mass remaining at the end of the wire was 0.5 tons. The tether end mass therefore decreases by a factor of twenty during the release. To avoid loss of tension, the reel maneuver used must reduce the tension to 5% of its original value with an uncertainty of less than 5% of the original value. In the initial study the maneuver was simulated by having the change in wire length given by the expression $-A\sin \omega t$ where ωt goes from 0° to 180°. In the results presented in the referenced report there was loss of tension in some segments of the wire after release of the payload, but the general approach seemed promising.

The present study is aimed at refining the algorithm used in the reel maneuver so as to develop a workable pre-release maneuver with particular emphasis on accounting for propagation delay and the dynamics of the tether itself in order to release the payload with no loss of

tension along the wire. The propagation delay is the time required for a sound wave to travel the length of the wire. In a solid material the velocity is $\sqrt{E/\rho}$ where E is the elasticity and ρ is the density of the material. For Kevlar, $E = 0.7 \times 10^{12}$ dynes-cm, and $\rho = 1.5$ grams/cc the speed of sound is about 6.8 km/sec. The propagation delay is therefore about 12 seconds for an 80 km wire. The physical properties of a braided Kevlar line could be significantly different than the properties of a monofilament and should be determined experimentally. The tether itself will oscillate as a result of a reeling maneuver and these oscillations will cause tension variations along the wire and at both ends.

The reel control algorithm can be defined in various ways. The previous study also contained some results obtained with a tension control algorithm. This technique gave low excitation of wire oscillations. However, such an algorithm does not give any direct control over wire length. The length control algorithm used in the previous study has the disadvantage that the beginning and ending of the reel maneuver are abrupt and result in needless excitation of wire oscillations. Two variations of the original length control algorithm have been tried in the present study. The change in length is given as $A(\cos \omega t - 1)$. If ωt goes from 0 to 360°, then maneuver pulls the wire in and then lets it out to the original length. If ωt goes from 0 to 180° the wire is only pulled in and the final wire length is shorter. In either case the rate of change of wire length is zero at the beginning and end of the maneuver so that the first derivative is continuous and there is less excitation of wire oscillations.

The objective of the reel maneuver is to pull the end mass toward the Shuttle and release the payload when the wire tension has been reduced to the value required for equilibrium after release. The reel maneuver must be completed before this minimum tension is achieved to avoid chaning the tension after release. The period of the reel maneuver must therefore be shorter than the natural period of oscillation of the subsatellite at the end of the wire. In the previous study it was assumed that the equilibrium tension is proportional to the mass at the end. In the case of a heavy payload, this assumption is not adequate because the center of gravity of the system undergoes a significant shift after release and the tension depends on the distance from the center of mass. This effect has been accounted for in the present study with improved results.

The response of the end mass to the reel maneuver cannot be calculated in a simple way. The approach used in this study is to start with a simple two-mass integration (neglecting wire dynamics). From the elastic properties of the wire we calculate the change in wire stretch required to bring the tension to the desired value for release of the payload. The amplitude of the reel maneuver is set to the desired change in wire stretch and a test run done with a two-mass model. If the amplitude of the response is so large so that the wire goes slack, the amplitude is reduced in the next run to eliminate loss of tension. The first parameter optimized is the period of the reel maneuver so that the maneuver finishes, with an adequate margin, before the minimum wire tension is achieved. The payload release is not included in these runs in order to determine the time of the minimum in the tension curve. For the two-mass model, either the tension or wire length can be used to determine the release time since the tension is linearly related to the

the wire length. Once the period is optimized, the amplitude is optimized by assuming that the response of the payload (that is, the change in distance from the Shuttle to the payload) is proportional to the amplitude of the reel maneuver. This assumption appears to be a good one when there is no loss of tension and the period of the reel maneuver is less than the natural period for longitudinal oscillations of the payload at the end of the wire. With the period and amplitude optimized, the payload is released and the tension variations examined in the post release time period. Very good results have been obtained for the tension fluctuations in the two-mass model since wire dynamics are neglected. In principle the tension fluctuations could be made arbitrarily small in the two-mass case by iterating the amplitude of the reel maneuver. In attempting to eliminate any tension variations after release it was found that the release time must be interpolated quadratically between output points in order to assure that the radial velocity of the subsatellite is zero. The velocity depends linearly on the error in release time and is therefore more critical than the position (and tension) which is a quadratic function of time near the minimum.

The next step in the analysis is to repeat the run adding wire masses and using the reel maneuver parameters from the two mass runs. The presence of wire masses has various effects such as shifting the center of gravity of the system (and altering the equilibrium tension as a result), introducing a delay in the propagation of tension signals between the Shuttle and subsatellite, and adding modelling of the longitudinal stress waves along the wire. For practical reasons it is not feasible to use large numbers of wire masses (such as 100) in the Skyhook program. Runs with up to 10 or 20 points can be done in a reasonable manner. The detailed results will depend on the number of mass points used in the model. The

approach taken in the study is to use the difference in results with various numbers of masses as a measure of the uncertainty introduced by the discrete modelling of the physically continuous wire. In particular the results with increasing number of mass points should not diverge in order to give confidence that the modelling of a particular problem is adequate. Wavelengths shorter than the spacing between mass points cannot be modelled. In the present study, the reel maneuver is of low frequency and has no sharp discontinuities which would introduce short wavelength effects.

In the multi-mass runs the first simulation is run without release of the payload to find the point of closest approach of the subsatellite. The tension plots are not useful for finding the release time because of the confusing effects of the longitudinal wire oscillations. A surprising result of the multi-mass run is that there seems to be almost no effect of propagation time on the response of the end mass. The time of closest approach of the subsatellite is only slightly later with the wire masses present than in the two-mass case which gives instant transmission of tension between the Shuttle and the subsatellite. The propagation time is short compared to the period of the reel maneuver. One may conjecture that the time of closest approach may depend on the root sum square of the period of the reel maneuver and the propagation time rather than on the algebraic sum of the two. Unfortunately, the present study does not allow time to study this effect in detail and determine how the behavior depends on the period and propagation time. The tentative conclusion is that propagation time can be ignored as long as it is short compared to the period of the reel maneuver.

Two types of plots have been used to analyze the output of the computer runs. In one, tension in each wire segment is plotted as a function of time in order to see the magnitude of the tension variations and make sure that there is no loss of tension at any point along the wire. In the other, the radial vs. in-plane configuration of the wire is plotted at each output point in order to show the dynamics of the wire and the subsatellite. In a direct plot of the radial vs. in-plane coordinates, the dynamics of the reel maneuver does not show up because the motions are small compared to the length of the wire. In order to make the motions visible on a plot, the file of radial components has been processed to remove most of the constant part of the radial component. When the plot is scaled to fill the page, the motions in the radial and in-plane directions are amplified so that they can be seen easily. The processing of the radial components consists of the following. The Skyhook program produces a file of radial components $R_I(t_J)$ where I is the mass index and t_J is the time index. A modified file R' is produced where R' is given by

$$R'_I(t_J) = R_I(t_J) - R_I(t_1) + (I-1)\ \Delta R.$$

The constant ΔR is chosen to be just large enough to prevent the plots for each mass from overlapping. In the case being studied the value of ΔR is on the order of 1 km and the original spacing between mass points is on the order of 10 or more km depending on the number of mass points used to represent the wire.

1.2 Results of Study

This study has analyzed and compared four different cases of a payload release. For a 2 mm wire, one reel maneuver using the equation -A sin wt has been done and two runs using the equation A(cos wt -1) have been done for the half wave and full wave cases. Since the maximum tension during the reel maneuver was close to the break strength, another run was done with a 3 mm wire and a full wave reel maneuver. The principle effect of wire diameter is to alter the natural period for longitudinal oscillations of the mass at the end of the wire. This requires using a faster reel maneuver with a smaller amplitude. Otherwise, the basic approach is the same. For the 2 mm wire with a full period reel maneuver simulations were done with 2, 3, 4, 5, 6, 7, 8, 9, and 10 masses in the model. For the 2 mm half wave maneuver, 2 mass and 5 mass runs have been done. For the -A sin wt reel maneuver, runs were done with 2 and 3 masses. For the 3 mm full wave case, 2 mass and 10 mass runs were done.

In order to simulate the reel maneuver and payload release the subroutines DIFFUN and TENSION have been modified. Subroutine DIFFUN reads the time for release of the payload and the mass remaining at the end of the tether after release. For times previous to release the subsatellite mass given on the normal input is used for mass number 2. After the release time the value for the remaining mass is used. Subroutine TENSION modifies the natural length of the wire segment next to the Shuttle according to the equation

$$\ell = \ell_0 - A \sin(\omega t + \phi) + A \sin(\phi)$$

where ℓ_0 is the natural length value in the normal input and the constant A, ω, and ϕ are read along with t_f by subroutine TENSION. For times greater than t_f the value of ℓ is computed with $t = t_f$.

As a starting point for the current analysis a simulation has been done with a reel maneuver given by -A sin ωt with ωt going for a half cycle. The amplitude A was determined from runs with a two mass model taking into account the effect of the shift in the center of mass on the equilibrium tension after payload release. A three mass simulation (one wire mass) was done using the parameters A = 933 meters, period = 104.7 seconds and release time = 141.8 seconds. As in the previous study, there is some loss of tension as shown in Figure 1a. The vertical axis is tension in dynes between each pair of mass points. The plotting symbol indicates the lower numbered mass of the pair. For the highest numbered mass, the tension is between that mass and the Shuttle which is mass number 1. Figure 1b shows the in-plane vs. radial configuration of the wire. The radial components have been altered by using a spacing of 1.5 km between the curves for each mass point. This allows the plot scale to be expanded so that the motions in the vertical and horizontal direction are easily visible. The dotted lines indicate loss of tension in the wire segment.

In the next case, the phase angle ϕ of the reel maneuver is set to -90° so that the algorithm is basically a cosine function rather than sine function. This eliminates the discontinuity in the first derivative at the start of the reel maneuver. In this run the reel maneuver goes for a half cycle so that the wire is pulled in but not let out again. The parameters for the run are A = 543 meters, period = 209 seconds, and release time = 230 seconds. The reeling maneuver stops at 104.7 seconds. Figure 2a shows the tension as a function of time with 5 masses used in the model. There is no loss of tension and the tension variation after payload

release is 27%. Figure 2b shows the radial vs. in-plane behavior. The curves are spaced 2 km apart in the vertical axis in order to obtain a convenient plot scale for making the motions easily visible.

The third case was run with a full-wave reel maneuver. The wire is pulled in and then let out again. The parameters of the run are A = 454 meters period = 139 seconds and release time = 159 seconds. Figure 3a shows the tension as a function of time and Figure 3b shows the in-plane vs. radial behavior with the curves separated by 1 km in the vertical axis. The tension variations after release are approximately 23%. Since the wire is a physically continuous system, which is being approximated by a set of discrete masses, it is important to provide an estimate of the uncertainty introduced by the modelling. For this reason, a set of runs with different numbers of masses in the model has been done for this particular case. The same parameters have been used for the reel maneuver in all cases. The table below shows the tension variation after payload release for each number of masses.

Number of Masses	% Tension Variation
2	1
3	81
4	51
5	23
6	50
7	57
8	55
10	55

The results for 2 masses is very low because wire excitations are not modelled. The highest tension variation was for 3 masses and the lowest for 5 masses. The value of 55% seems to be the best estimate and is fairly consistent for the larger numbers of masses, none of the runs show loss of tension in any of the wire segments. Figure 4 shows the results with 10 masses in the model. Part a) is the tension vs. time and part b) is the in-plane vs. radial configuration with 1 km spacing between the plots for each mass.

With a 2 mm diameter wire, the maximum tension induced by the reel maneuver is close to the break strength of the wire. Therefore, one final run was done with a 3 mm wire to provide results for a physically realistic case. The wire diameter affects the stiffness of the wire and therefore the natural frequency of the oscillations of the payload at the end. The period for the reel maneuver had to be reduced to keep it shorter than the response time of the end mass. Figure 5a shows the tension variation vs. time and Figure 5b shows the in-plane vs. radial with the curves separated by 9 km. There is no loss of tension but the parameters are not optimized and there is an oscillation of the payload after release in addition to the wire oscillation. Unfortunately there was not sufficient time to find the cause of the problem and refine the parameters. One problem may be the fact that the wire mass is larger and the wire mass was not included in the center of mass calculations. The parameters used in the run are A = 176.6 meters, period = 114.5 seconds, and release time = 117 seconds.

The major problem in the cases studied is the tension variations caused by longitudinal oscillations of the tether. The techniques developed in this study give satisfactory behavior for a case which is difficult because of the large ratio of the tension before release to the tension after release.

The technique could be refined if necessary by developing an algorithm whereby the reel motor is used to damp longitudinal oscillations of the tether. Such an algorithm would have to be written as a function of the observables available at the reel motor such as tension and deployed tether length. The derivatives of these quantities could also be available by measuring the quantities at appropriate intervals. Such an algorithm would be of general usefulness in many tether operations.

The most unexpected feature of the simulations is the apparent absence of propagation delay in the response of the end mass. It would be interesting to study this effect in more detail to understand how is depends on the various time constants in the dynamics of the system such as the natural frequency of oscillation of the end mass, the period of the reel maneuver, and the speed of sound along the wire. A one-dimensional program exists which could be fairly easily modified for use in such a study. By adding the gravity gradient force to this program, the propagation delay could be efficiently studied with the increased resolution provided by the larger number of mass that can be handled.

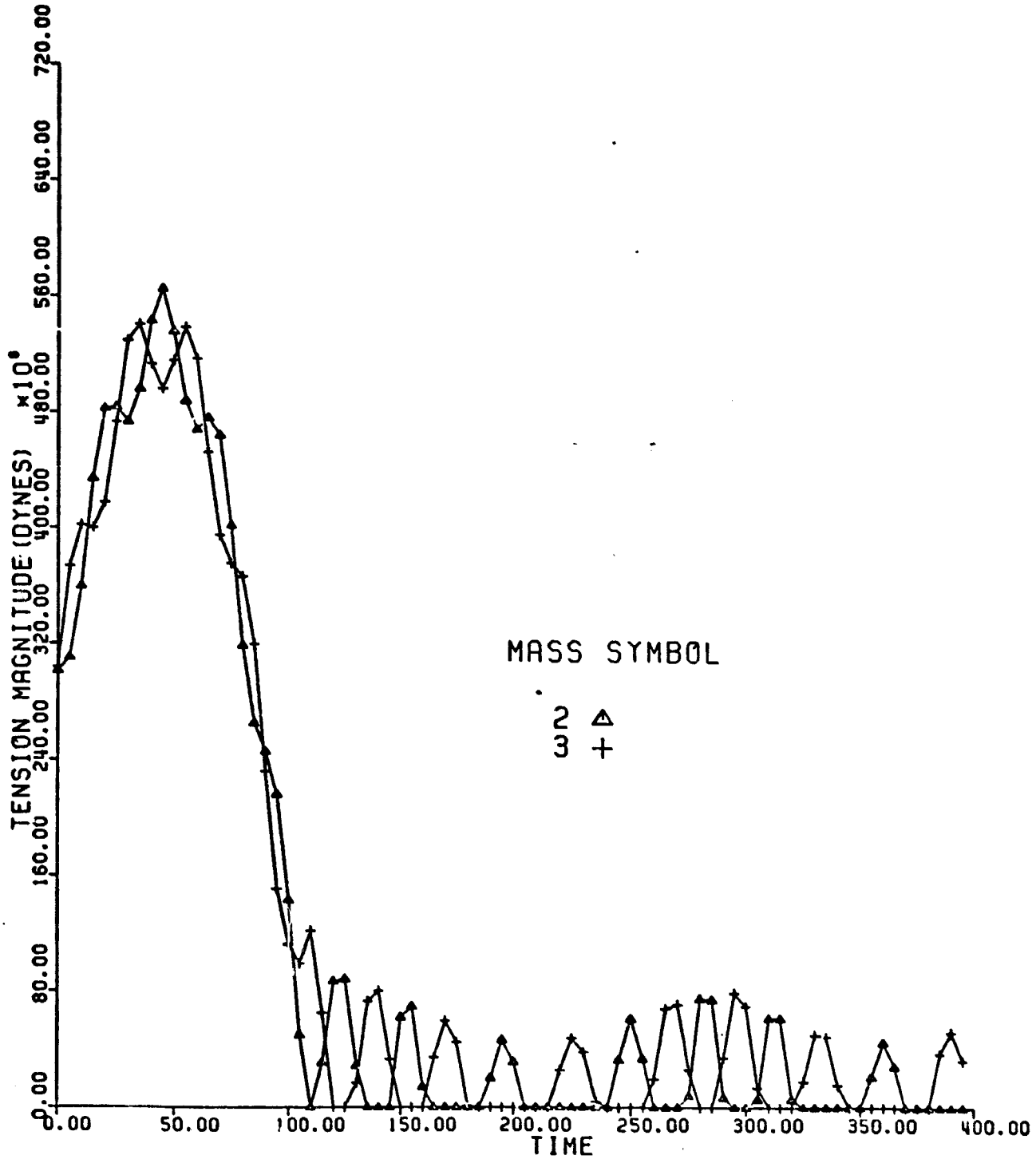

Figure 1a

ORIGINAL PAGE IS
OF POOR QUALITY

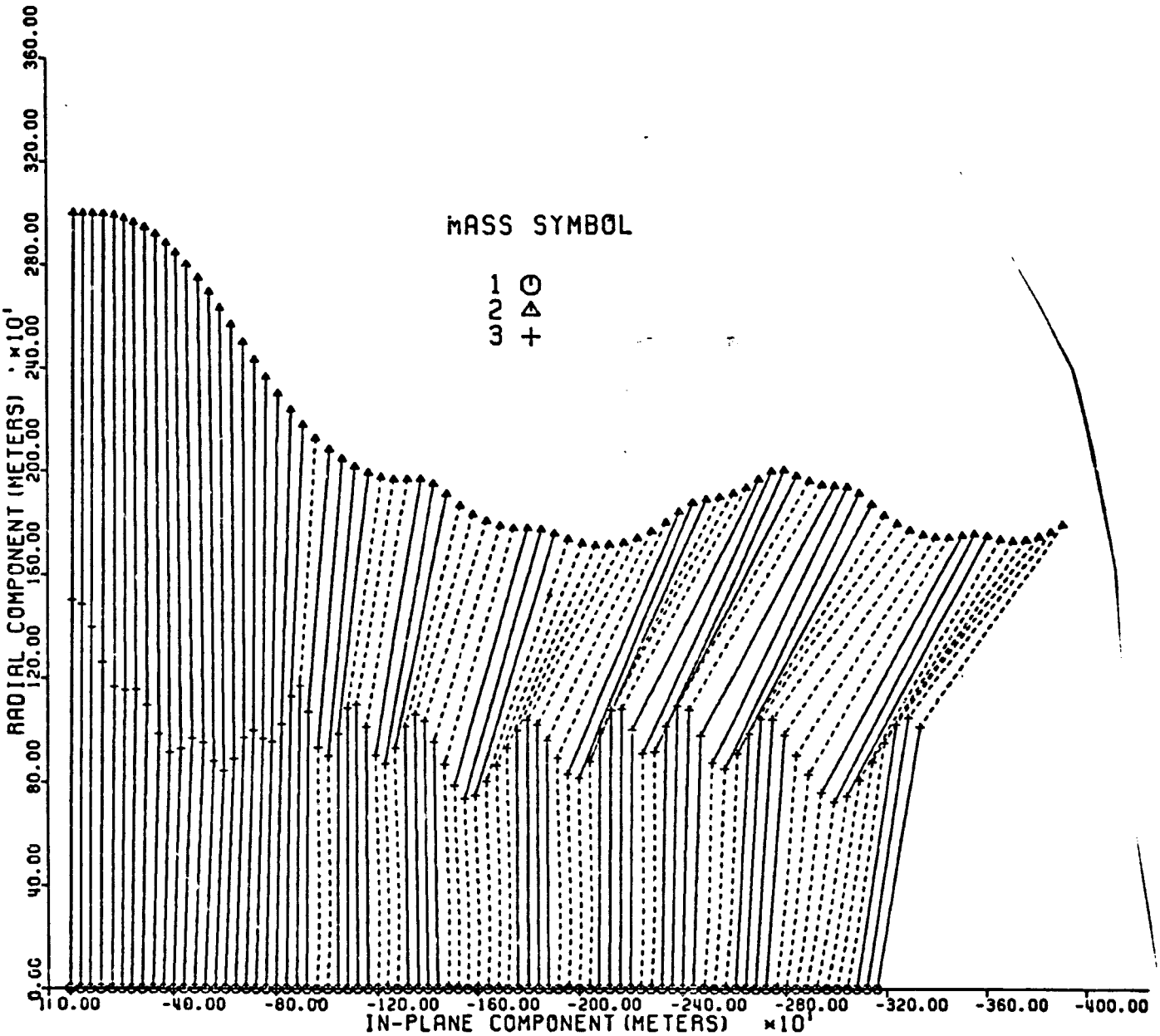

Figure 1b

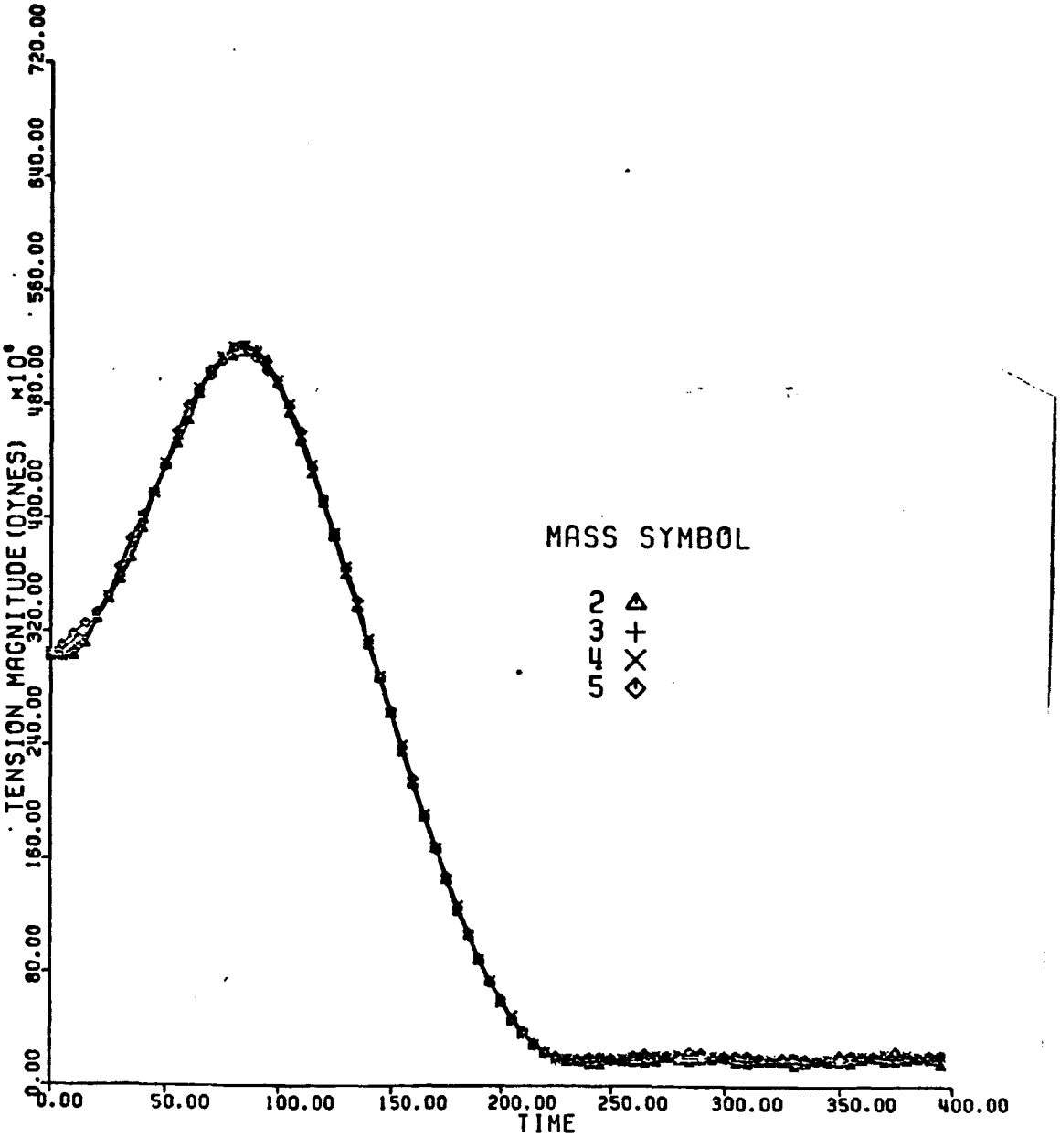

Figure 2a

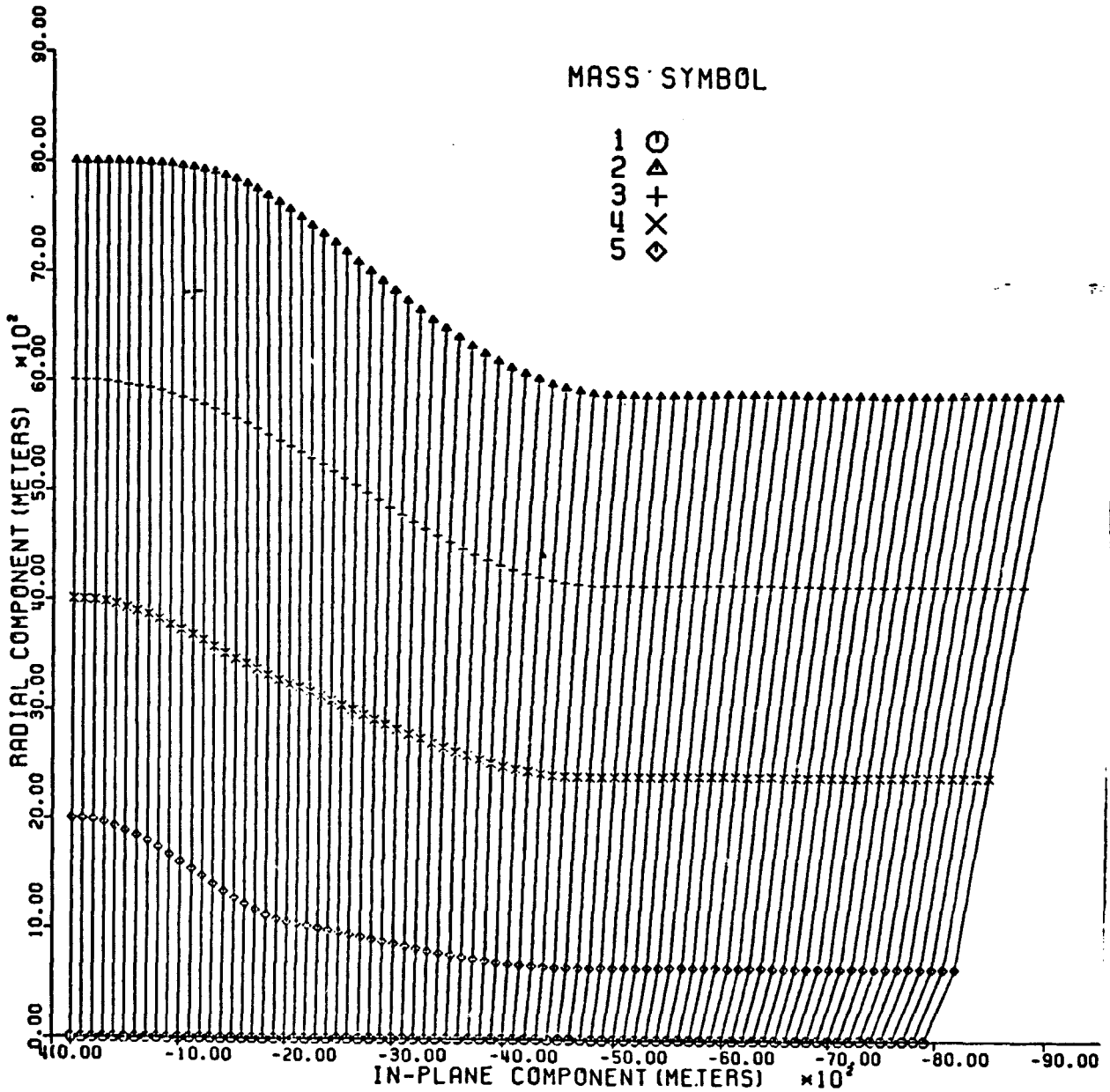

Figure 2b

ORIGINAL PAGE IS
OF POOR QUALITY

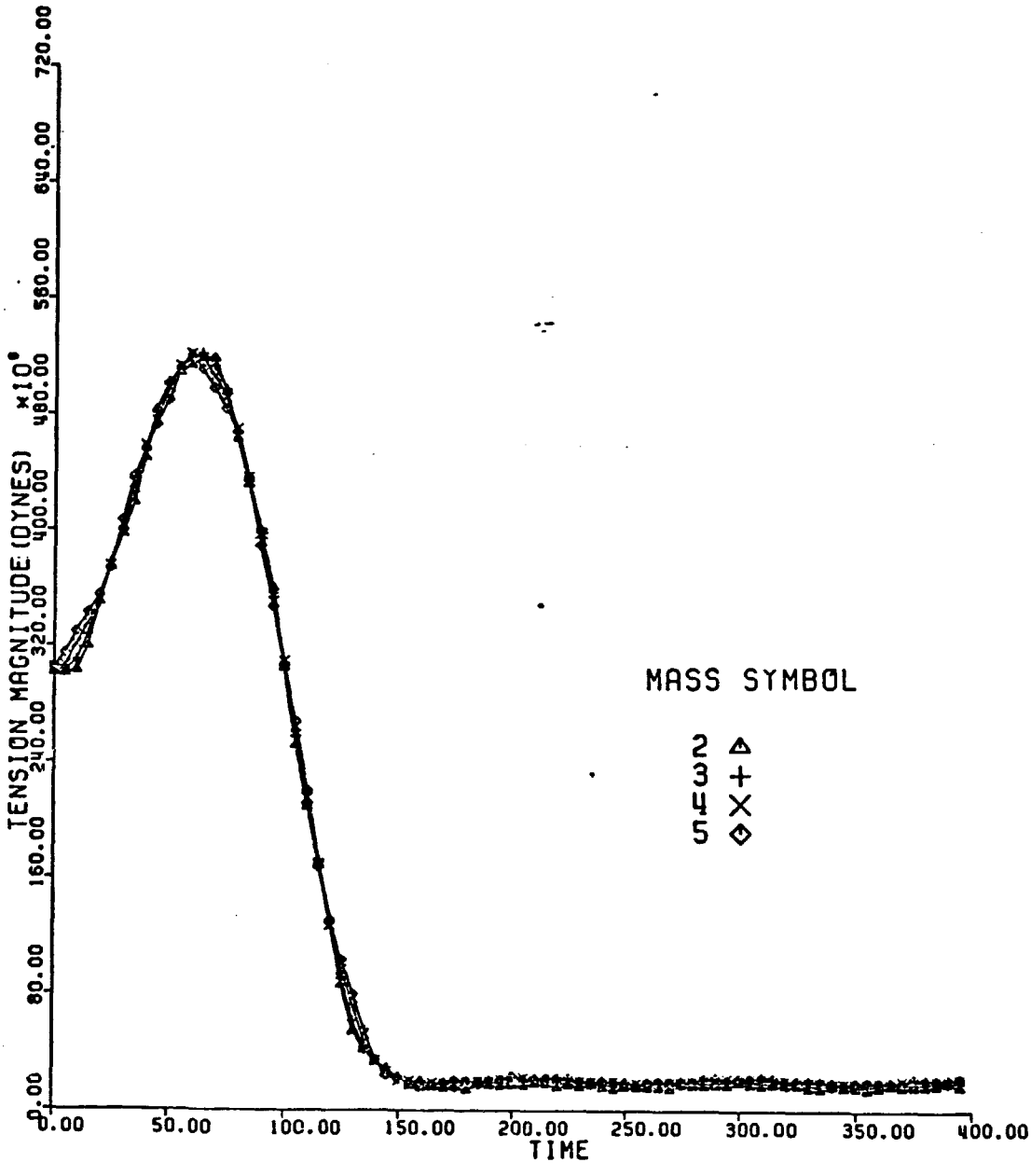

Figure 3a

ORIGINAL PAGE IS
OF POOR QUALITY

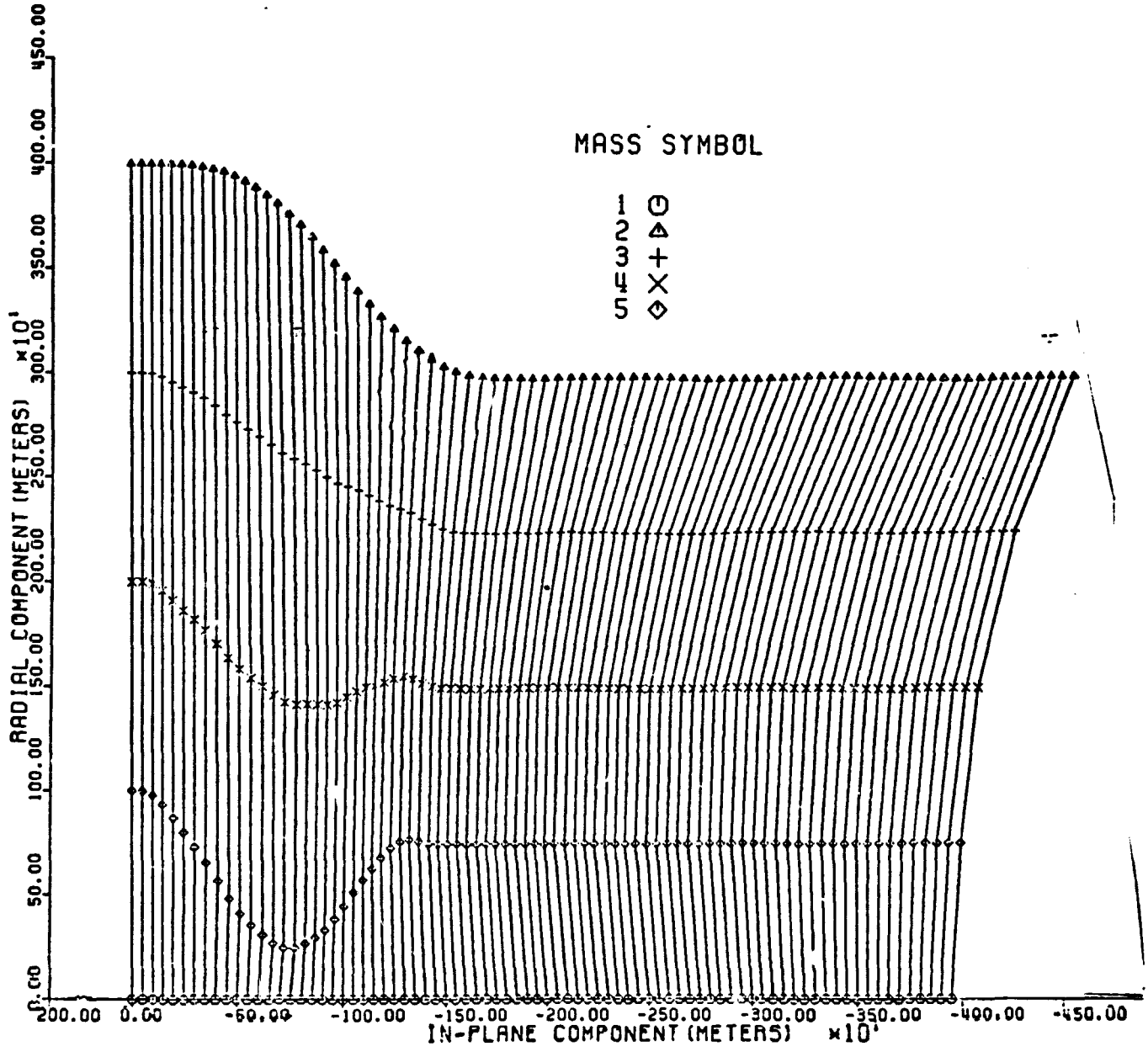

Figure 3b

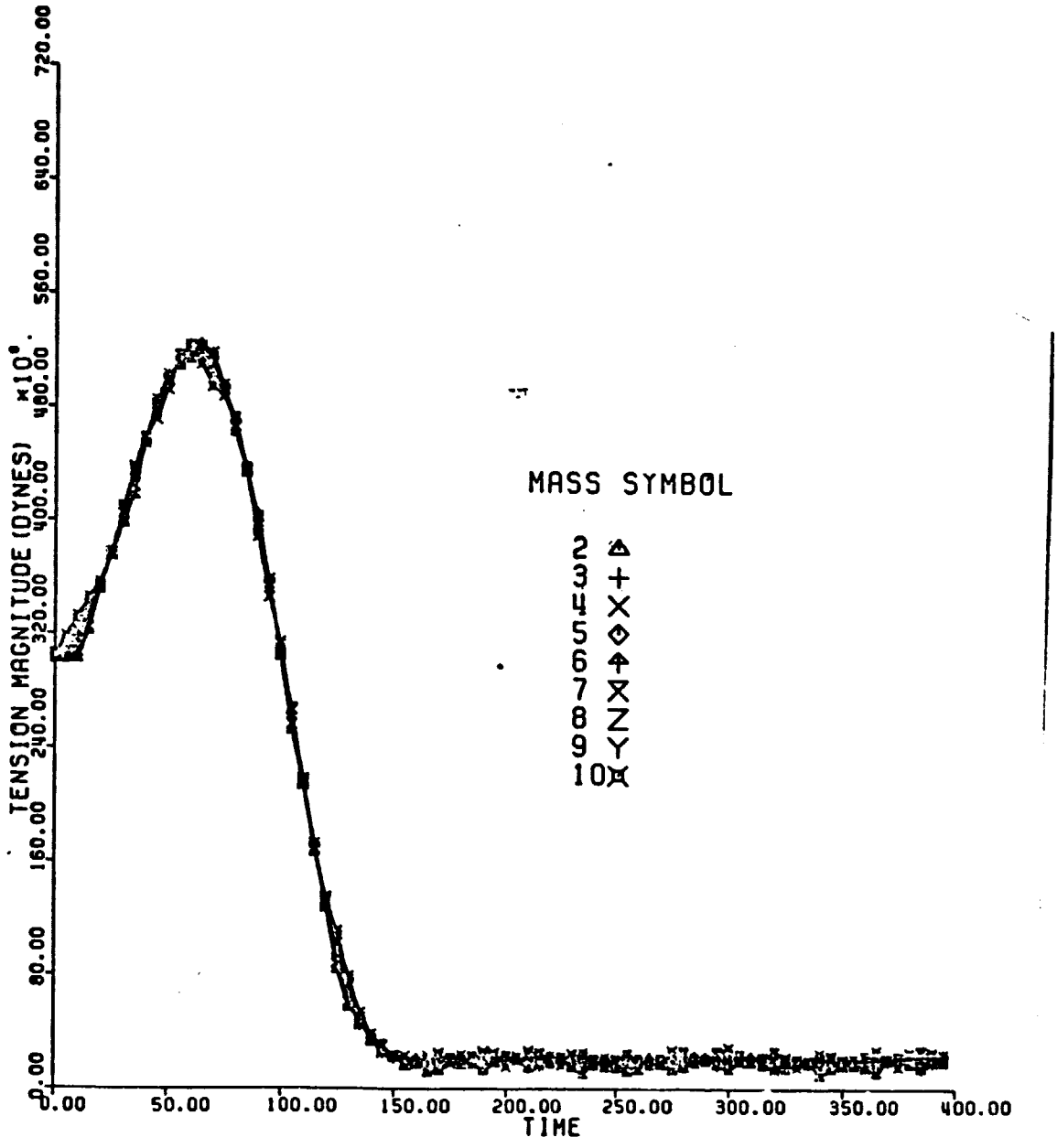

Figure 4a

ORIGINAL PAGE IS
OF POOR QUALITY

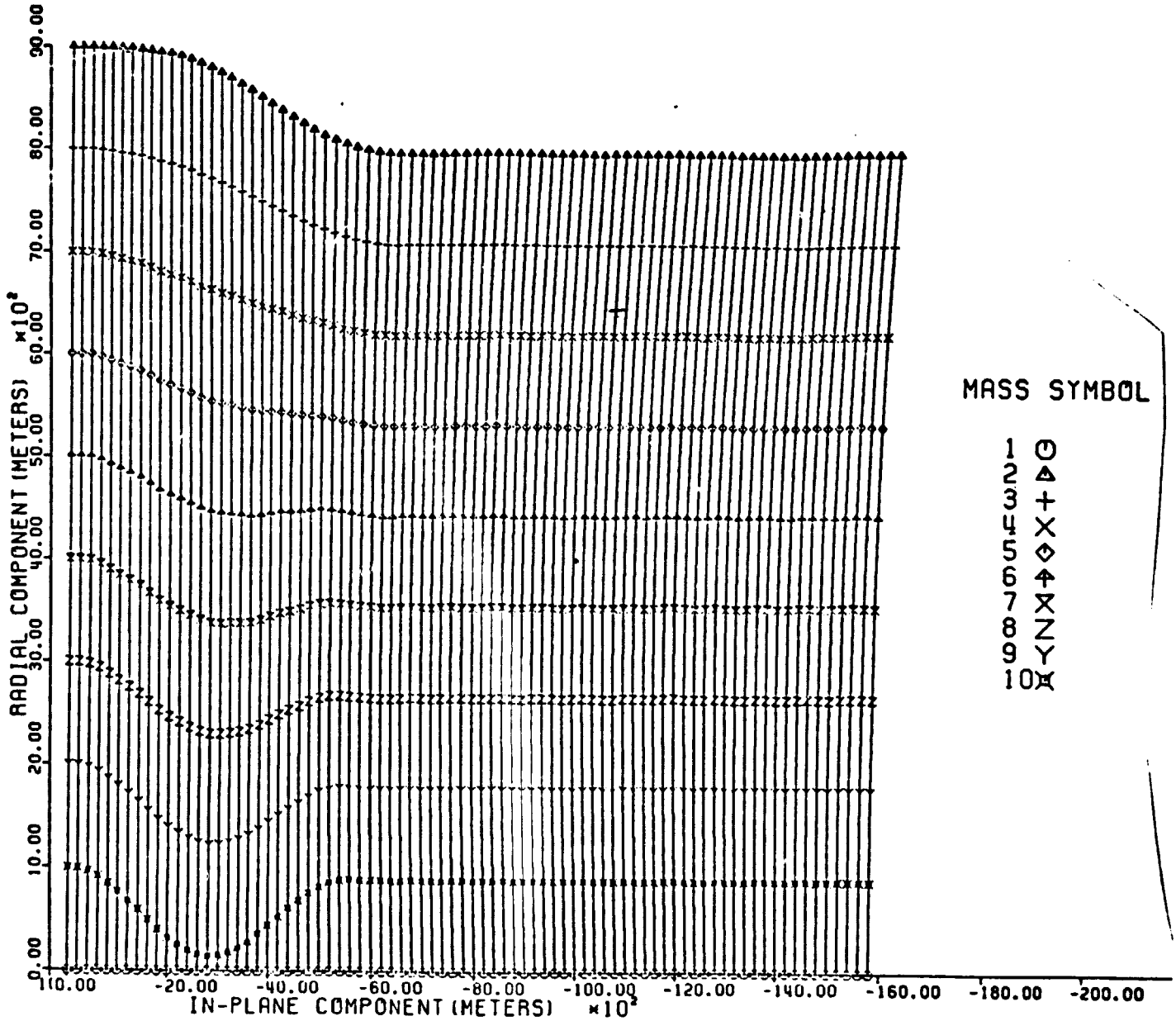

Figure 4b

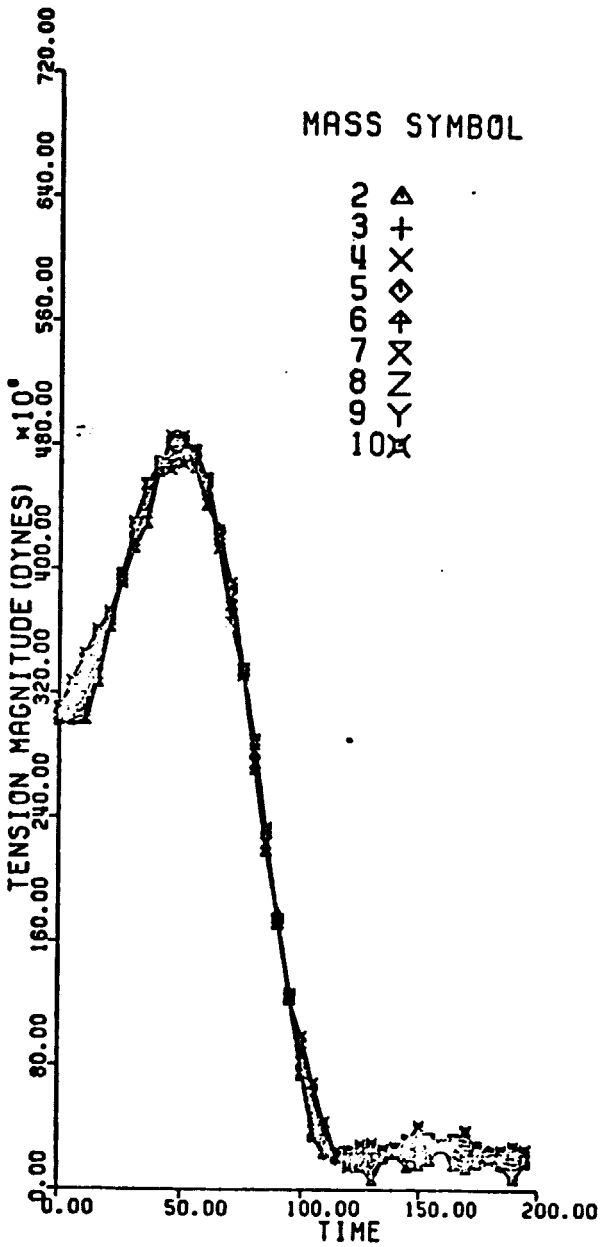

Figure 5a

ORIGINAL PAGE IS
OF POOR QUALITY

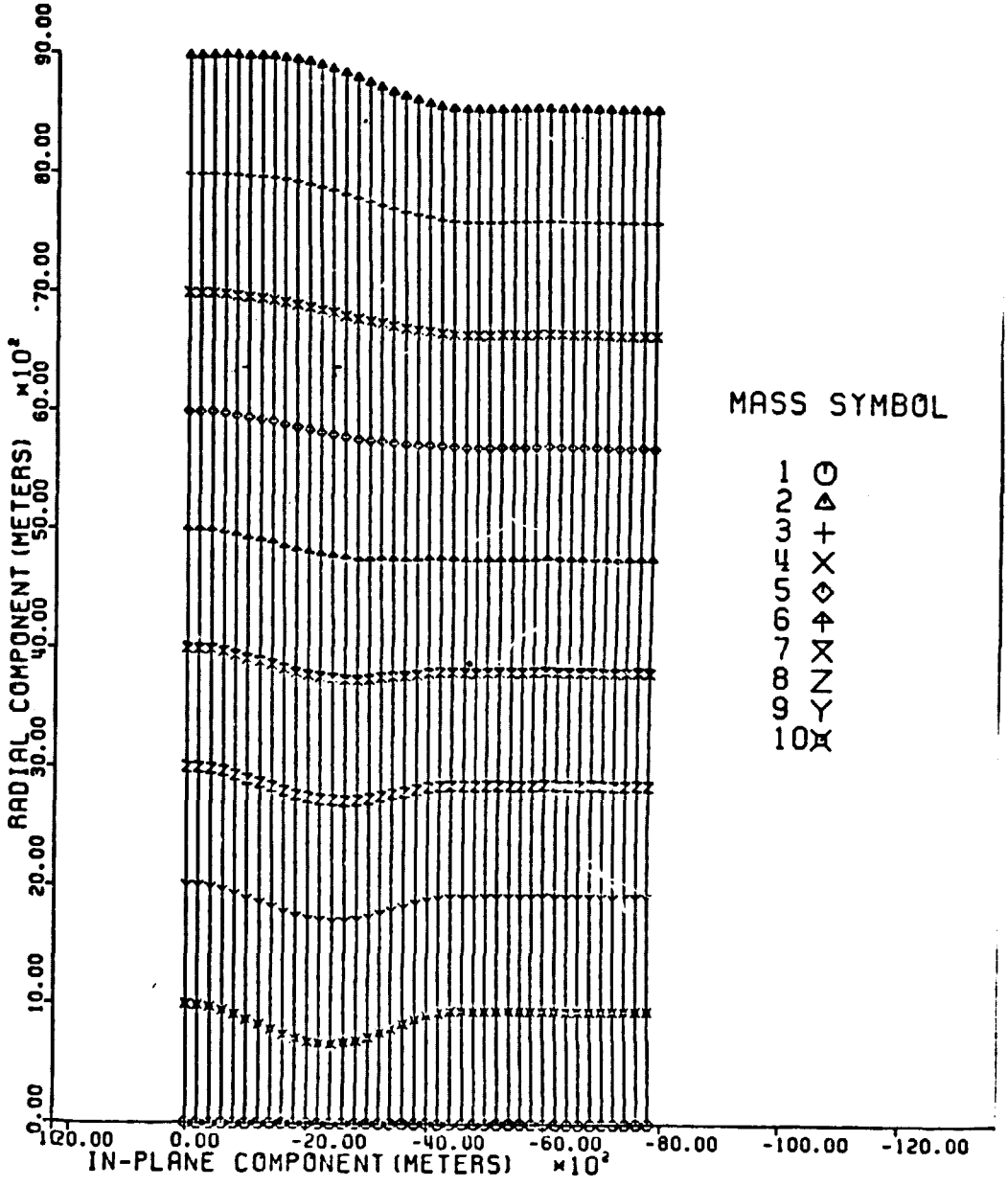

Figure 5b

Appendix

Space Based Tethers as Extensions of the Space Transportation System for LEO-GEO Transfers

Dr. Manuel Martinez-Sanchez

Co-Investigator

Space-based Tethers as Extensions of the Space Transportation System for LEO-GEO Transfers

1. Introduction. In our previous monthly report (Ref. 1) we examined in some depth the possibility of using a tether system on board the Space Shuttle as an aid in launching satellites into GEO-bound transfer orbits. It was assumed that the maximum throw-weight of the Orbiter was always utilized (including the OTV with its payload, the tether system and the on-board OMS fuel), and that the Shuttle delivered the payload using the on-board tether to as low an orbit as possible, without itself being forced to altitudes below 100 n.m. The full tether system (lower and upper pallets plus rewound tether) was returned to Earth after each mission. It was concluded on the basis of the calculations performed that this system could not deliver as much payload to GEO as the baseline system without tethers. The difficulty was traced to two main points: (a) For short tethers (below some 100 km), the dominant effect was the extra OMS fuel required for the Shuttle to achieve the required delivery height; since the throw weight was limited, this extra was reflected in a smaller payload. (b) For long tethers, the need to carry a massive tether system to and from orbit became dominant and, again, detracted from payload.

In the present report we investigate the effects of removing one of these constraints, namely, the transportation of the tether system. This is accomplished by leaving this system in orbit, in a manner described and analyzed in Ref. 2. We perform the corresponding calculations for two limiting cases: (a) Full throw weight utilization (similar to our study for the Shuttle-based tether system). This implies a different OTV size for each choice of tether

length or other parameters; as such, it represents a maximum payload envelope, and is appropriate for system definition studies.

(b) Fixed Orbital Transfer Vehicle, maximum OMS fuel use. This case corresponds more closely to a practical situation where a particular OTV, such as some modified Centaur, is available, and the Shuttle cargo capacity is not completely used up by this OTV plus its payload. Here the tether can be viewed as a boost to the OTV, rather than a partial substitute.

2. Notation. The following notation is used in the analysis:

L	tether length (full)
ℓ	tether length (partially rewound)
x	for a deployed tether, distance from its lower end to the c.g. of the tether-platform-payload system
x'	same, but to the c.g. of the tether system alone
$\tilde{x}'$	same as x', but after partial rewinding
R_{LEO}, h_{LEO}	radius and altitude to the initial (and final) orbit of the tether system
R_{MIN}, h_{MIN}	Minimum radius and altitude for the Orbiter (set at 100 n.m.). For case (a), this is also the altitude from which the Orbiter will reenter.
$\Delta V_{inj,rm}$	Shuttle velocity increments from MECO to attain parking orbit at h_{MIN}, and for reserve and maneuvering. Taken as 92.5 m/sec.
ΔV_{tr}	ΔV for transfer from parking orbit to tether system orbit, at h_{LEO}
ΔV_{deorb}	Deorbiting ΔV for Shuttle
$\mu = 1 - e^{-\Delta V/c_{OMS}} \simeq \Delta V/c_{OMS}$	, where $c_{OMS} = g(I_{sp})_{OMS}$ is the effective jet speed for the OMS rockets (taken as 9.8x313 m/sec)
M_{OMS}	Mass of OMS fuel needed on the Shuttle. Limited to 24,000 lb
M_L	Loaded OTV mass (including payload)
M_{throw}	Shuttle throw weight, limited to 90,000 lb. Since the tether system is left in orbit, we take $M_{throw} = M_{OMS} + M_L$

M_T tether mass

M_{up}, M_{Lp} masses of the upper and lower pallets at the tether ends. M_{up} taken to be 2000 Kg. M_{Lp} variable.

$M_{TS} = M_T + M_{up} + M_{Lp}$ tether system mass

ΔV_1, ΔV_2, ΔV perigee, apogee and total velocity increments supplied by OTV. No change of plane assumed

M_{p_2}, $M_{OTV,s}$, M_{pay} - OTV propellant, OTV structural mass and carried payload (to Geosynchronous orbit).

(SF) - safety factor for tether material. Nominal value = 3.

σ - break strength of tether. Taken as 1.4×10^9 N/m^2

ρ - density of tether material taken as 1440 Kg/m^3

3. Discussion and Results for Case (a) (Full Throw Weight)

The sequence of events here is:

(a) The tether system has been orbited to the appropriate altitude (corresponding, as will be seen, to a given tether length, and other system parameters).

(b) The Shuttle goes from MECO to parking orbit, then to the tether orbit, and docks with the Lower Pallet.

(c) Tether unwinds with the OTV at its end. After stabilization, OTV is released.

(d) Partial rewinding of tether (to length $\ell < L$) from the Shuttle, then the Shuttle detaches. Rewinding completed from Lower Pallet. Tether system is back in original orbit.

(e) Shuttle, after detaching, is in elliptic orbit with perigee at h_{MIN}. Deorbiting burn applied at one apogee passage.

The size of the Orbital Transfer Vehicle is here assumed variable, and is always selected such as to fully utilize the available throw weight capacity:

$$M_{OMS} + M_L = (M_{throw})_{MAX} \qquad (1)$$

The payload, fuel and structural masses making up M_L are then apportioned according to the required ΔV for transfer to GEO and the prescribed structure/fuel ratio for the OTV. The ΔV itself depends on the altitude and speed of the payload at the instant of release from the tether; thus all of the variables interact with each other and an iterative calculation is required. The algorithm used was as follows:

(1) Select inputs: $(M_{throw})_{MAX}$, $M_{Shuttle,empty}$, $\Delta V_{inj,rm}$, c_{OMS} , c_{OTV} , $M_{OTV,s}/M_{p_2}$, M_{up} , L

(2) Guess x/L , $\frac{x'-\tilde{x}'}{L}$.

(3) $R_{LEO} = R_{min} + 7\ L\ (\frac{x}{L} - \frac{x'-\tilde{x}'}{L})$ (from Ref. 1)

(4) $f = 1 + \frac{L}{R_{LEO}}(1 - \frac{x}{L})$; $\rho = \frac{R_{GEO}}{R_{LEO}}$; $\eta = 1 - \frac{R_{min}}{R_{LEO}}$; $v_{cp} = \sqrt{\frac{\mu_e}{R_{min}}}$

$$\Delta V_1 = \frac{v_{cp}}{\sqrt{1+\eta}}\left(\sqrt{\frac{2\rho}{f(f+\rho)}} - f\right) \quad ; \quad \Delta V_2 = \frac{v_{cp}}{\sqrt{1+\eta}}\left(1 - \sqrt{\frac{2f}{f+\rho}}\right)$$

$\Delta V = \Delta V_1 + \Delta V_2$ (from Ref. 3)

(5) $\mu_{inj,rm} = \frac{\Delta V_{inj,rm}}{c_{OMS}}$; $\mu_{tr} = \frac{v_{cp}}{c_{OMS}}\ \frac{\eta}{2}$; $\mu_{deorb} = \frac{v_{cp}}{c_{OMS}}\ \frac{1}{4}\ \frac{h_{min}}{R_E}$

$$(6)\quad M_L = \frac{M_{throw} - M_{SH,E}(\mu_{inj,rm} + \mu_{tr} + \mu_{deorb})}{1 + \mu_{inj,rm} + \mu_{Er}}$$

$$(7)\quad M_{p_2} = M_L(1 - e^{-\Delta V/c_{OTV}}) \qquad M_{OTV,s} = \left(\frac{M_{OTV,s}}{M_{p_2}}\right) M_{p_2}$$

$$M_{pay} = M_L - M_{p_2} - M_{OTV,s}$$

$$(8)\quad \gamma^2 = \frac{3}{2}\frac{\mu_0 L^2}{\sigma R_{LEO}^3} = 6.14\times10^8 \frac{(SF)L^2}{R_{LEO}^3} \qquad \nu = \frac{M_{up} + M_L}{M_{sh}}$$

$$M_T = (M_{up} + M_L)\frac{2\gamma^2}{1+\nu} e^{\frac{\gamma^2}{(1+\nu)^2}} \qquad \text{(Ref. 4)}$$

$$(9)\quad M_{LP} = 2000 + 1.5\, M_T$$

$$(10)\quad M_{TS} = M_{Lp} + M_T + M_{up} \quad ; \quad M_{TOT} = M_{SH} + M_{ts} + M_L$$

$$(11)\quad \frac{\ell}{L} = -\frac{M_{up}}{M_T} + \sqrt{\left(\frac{M_{up}}{M_T}\right)^2 + 2\frac{M_L}{M_{TOT}}\frac{M_{TS}}{M_T}\frac{M_{SH,E} + M_{LP} + M_T/2}{M_{SH,E}}} \qquad \text{(Ref.2)}$$

$$(12)\quad \frac{x}{L} = \frac{M_L + M_{up} + M_T/2}{M_{TOT}} \quad ; \quad \frac{x'-\tilde{x}'}{L} = \frac{1}{2}\frac{M_T(1-\ell/L)}{M_{TOT} - M_L} \qquad \text{(Ref.2)}$$

(13) Compare to assumed values; iterate to convergence

The results of these calculations are summarized in Figs. 1, 2 and 3. Fixed parameters were

h_{MIN} = 182 Km (v_{cp} = 7793.9 m/sec)

M_{up} = 2000 Kg , SF = 3

$(M_{throw})_{MAX}$ = 90,000 lb , $M_{SH,E}$ = 80,000 Kg

$M_{p_2}/M_{OTV,s}$ = 6.826

I_{sp} = 313 sec , I_{sp} = 460 sec

The most important result in Fig. 1 is the fact that the payload mass M_{PAY} decreases with tether length L, although much less than was the case in the similar calculations for Shuttle-carried tether systems (Ref.1). Increasing L does allow a reduction in both fuel and structural OTV masses (see Fig.1), but the increase in required OMS Shuttle fuel is still enough to offset these gains. Also shown in Fig. 1 are the tether and tether system masses; this mass is not a penalty in this case, since it will stay in orbit. Depending on tether length, the mass of this "mini-space station" goes from 4000 to some 15000 Kg. It can also be seen that throughout the range investigated ($L \lesssim 160$ Km), the assumed OMS tankage capacity of 24,000 lb. is not exceeded.

From a fundamental point of view, the result that the payload is reduced by the use of a tether could be anticipated. In Ref. 2 it was shown that, to first order, the amount of fuel used to recover the perturbed orbit of the tether reaction mass after payload release is the same as that saved by the payload propulsion system due to the tether boost if the two propulsion systems have equal specific impulses. Here we do not exactly restore the perturbed orbit, since the Shuttle eventually reenters from an elliptic orbit different than the initial, circular one. However, we can expect that the use of the low specific impulse OMS rockets to supply the required orbital boosts for the Shuttle will always be disadvantageous when compared to the capabilities of enlarged OTV engines, with their higher specific impulse. Once again, this points at the desirability of using high specific impulse electric propulsion for restoring the perturbed orbits, such as discussed in Ref. 5. Alternatively, tethers can be used as supplements to, rather than as substitutes for chemical propulsion stages (see Section 4 of this Report).

The underlying reason for the large OMS fuel increase is the need to fly the Shuttle to higher orbits than the minimum altitude orbit at h_{MIN}. This is illustrated in Fig. 2, which shows the altitude required for the tether system - for each tether length.

As indicated in the discussion, the tether is partially rewound from the Shuttle before the latter detaches, in order to restore the tether system to its original orbit. Fig. 3 shows the fraction ℓ/L left for autonomous rewinding. It can be seen in Fig. 3 that for lengths beyond some 123 Km, it becomes impossible to restore the initial tether orbit, unless some additional unwinding is done after tether release. This would probably be only a minor difficulty, however.

Some additional calculations were performed to learn about the sensitivity of these results to various parameter variations. A brief discussion is given of each of these.

(a) Assuming the OMS system could be made to operate on LOX-LH_2 fuel (I_{sp} = 460 sec), just as the OTV itself, we find for tether lengths of 0 and 100 Km the following results:

L (Km)	0	100
M_{pay}(Kg)	12,413	12,276

Thus, even with this favorable assumption there is a slight performance loss due to the tether. This must be ascribed to the incomplete restoration of the reaction mass to its initial state, i.e., the Shuttle actually takes away some extra momentum that could have gone to the payload.

(b) With I_{OMS} back at 313 sec, if the upper pallet mass is increased from 2000 to 4000 Kg, for L = 100 Km, the payload is reduced from 11,340 Kg

to 11,304 Kg, while the fraction ℓ/L decreases substantially (from 0.948 to 0.739).

(c) With M_{up} back at 2000 Kg, variations in the assumed tether safety factor have the following effects (for L = 100 Km):

SF	2	3	4
M_{pay}(Kg)	11,334	11,340	11,345
M_T(Kg)	1,932	2,929	3,946
h_{LEO}(Km)	383.8	383	382.3
ℓ/L	0.877	0.948	0.995

Thus, curiously enough, heavier tethers ensure higher payload mass.

(d) A similar effect was found by arbitrarily increasing the lower pallet mass from 2000 + 1.5 M_T to 4000 + 1.5 M_T . This increased the payload from the base value of 11,340 Kg to 11,353 Kg. At the same time it required ℓ/L = 1.068 (up from 0.948).

4. Discussion and Results for Case (b) (Fixed OTV)

Here the propellant and structural masses of the Orbital Transfer Vehicle were arbitrarily fixed at the values (corresponding to one version of the Centaur vehicle)

$$M_{p_2} = 10{,}870 \text{ Kg} \qquad M_{OTV,s} = 3230 \text{ Kg}$$

Given this condition, the largest payload to GEO can be secured by using the full OMS fuel complement of the Shuttle, for any tether length (or without tether). This was therefore assumed for the calculations in this section. Correspondingly, the perigee altitude of the Shuttle after

releasing the tether is no longer constrained to be h_{MIN} , only to be above this leve (at an altitude called h_{deorb}). Also, the throw weight is in this case below its maximum value, corresponding to the notion of a partially loaded Shuttle.

The calculation procedure used in this case was as follows:

(1) Select fixed parameters (as in Case (a), except that M_{OMS}, M_{p_2} and $M_{OTV,s}$ are fixed, and M_{throw} is not)

(2) Guess $\frac{x}{L}$, $\frac{x'-\tilde{x}'}{L}$ and h_{deorb} .

(3) $R_{LEO} = R_{deorb} + 7\ L\ (\frac{x}{L} + \frac{x'-\tilde{x}'}{L})$

(4) Calculate f, ρ , η , ΔV_1, ΔV_2, ΔV , as in case (a)

(5) $\mu_{inj,rm} = \frac{\Delta V_{inj,rm}}{c_{OMS}}$; $\mu_{tr} = \frac{v_{cp}}{c_{OMS}} \frac{\eta}{2}$; $\mu_{deorb} = \frac{v_{cp}}{c_{OMS}} \frac{h_{deorb}}{4\ R_E}$

(6) $(M_L)^{(1)} = \frac{M_{p_2}}{1 - e^{\Delta V/c_{OTV}}}$. $M_L^{(2)} = \frac{M_{OMS} - M_{SH,E}\ \mu_{deorb}}{\mu_{inj,rm} + \mu_{tr}} - M_{SH,E}$

(7) Compare $M_L^{(1)}$ to $M_L^{(2)}$. If not equal, select new h_{deorb}, iterate.

(8) $M_{pay} = M_L - M_{p_2} - M_{OTV,s}$

Steps (9) and beyond are as in Case (a). Eventually a new set of values of $\frac{x}{L}$, $\frac{x'-\tilde{x}'}{L}$ is generated, which must agree with the initial guess. This is ensured by an outer iteration loop.

The results using M_{OMS} = 24,000 lbs are presented in Figs 4,5 and 6. In Fig. 4 the essential result is the increase of M_{pay} with tether length.

This is as expected, since the tether system acts now as a supplementary booster over and above the fixed OTV. The increase amounts to a 12% per 100 Km of tether, and may make this a practical option for expanding the capabilities of an otherwise fixed Space Transportation System.

The other masses of interest are also displayed in Fig. 4. As indicated, the sum of M_L and M_{OMS} never exceeds the maximum throw weight of 90,000 lb. Fig. 5 shows the required orbital altitude for the tether system (h_{LEO}) and the corresponding minimum perigee (h_{deorb}) of the Shuttle. This latter altitude is always above the minimum of 183 Km. Also, the tether system altitude ranges from 425 to 489 Km, which is high enough to make drag effects negligible on the orbiting system.

The partial rewinding length ℓ is shown in Fig. 6. In this case the fraction ℓ/L is always less than unity, which makes it always possible to restore the tether system orbit.

5. Summary and Conclusions

(a) Unless high specific impulse engines can be used to restore the orbit of the tether platform, tethers cannot advantageously be used to replace part of the chemical propulsion capacity of an OTV.

(b) For a system where the Shuttle is fully loaded with either the largest possible OTV, or a smaller OTV plus additional OMS fuel to reach a tether system at its minimum altitude (compatible with no Shuttle reentry upon release), there is a loss of 4.7% payload per 100 Km of tether.

(c) However, tethers can be used to extend the capacity of a fixed OTV. For a system where the Shuttle carries a Centaur OTV, to a tether system orbiting as high as the maximum OMS fuel will allow, there is gain of 12% per 100 Km of tether.

References

(1) "An Assessment of Shuttle-Based Tethers for Geosynchronous Transfer Assist." Monthly Progress Report for Sept. 1982, from M.I.T. Space Systems Lab to the Smithsonian Astrophysical Observatory, Subcontract SV2-52005 on NASA Contract No. NAS8-33691.

(2) "The Use of Tethers for Payload Orbital Transfer." Final Report on Subcontract SV1-52006. Submitted to the SAO by M.I.T. Space Systems Lab, March 22, 1982 (Chapter 3).

(3) Ibid, Sec. 4.2.

(4) Ibid, Appendix 1.

(5) Ibid, Chapter 4.

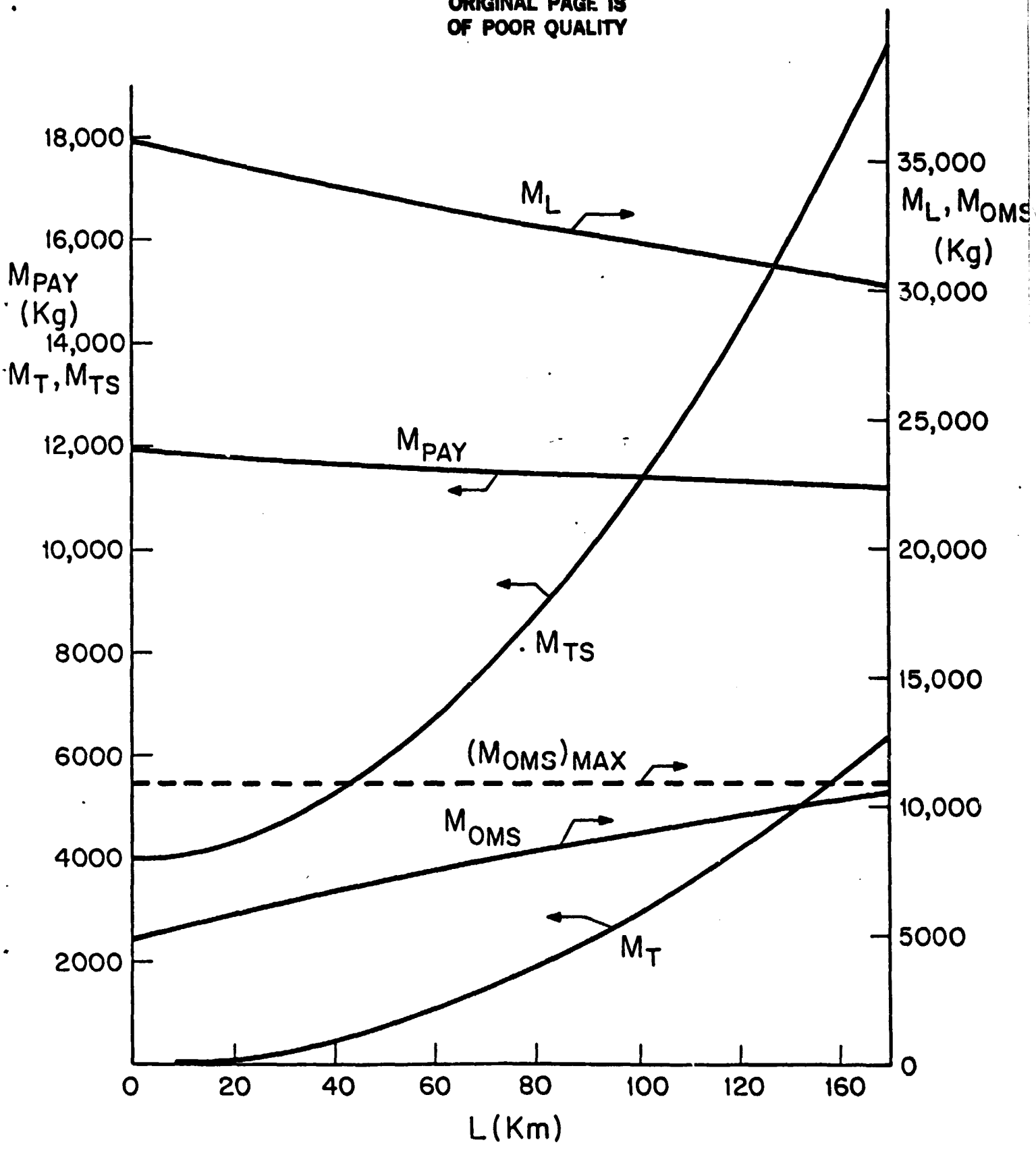

Fig. 1 Case with Throw Weight Limited to 40,770 Kg.
Variation of payload, tether and tether system masses (left scale), and of loaded OTV and OMS Orbiter fuel (right scale) with tether length. Minimum altitude 100 nm.

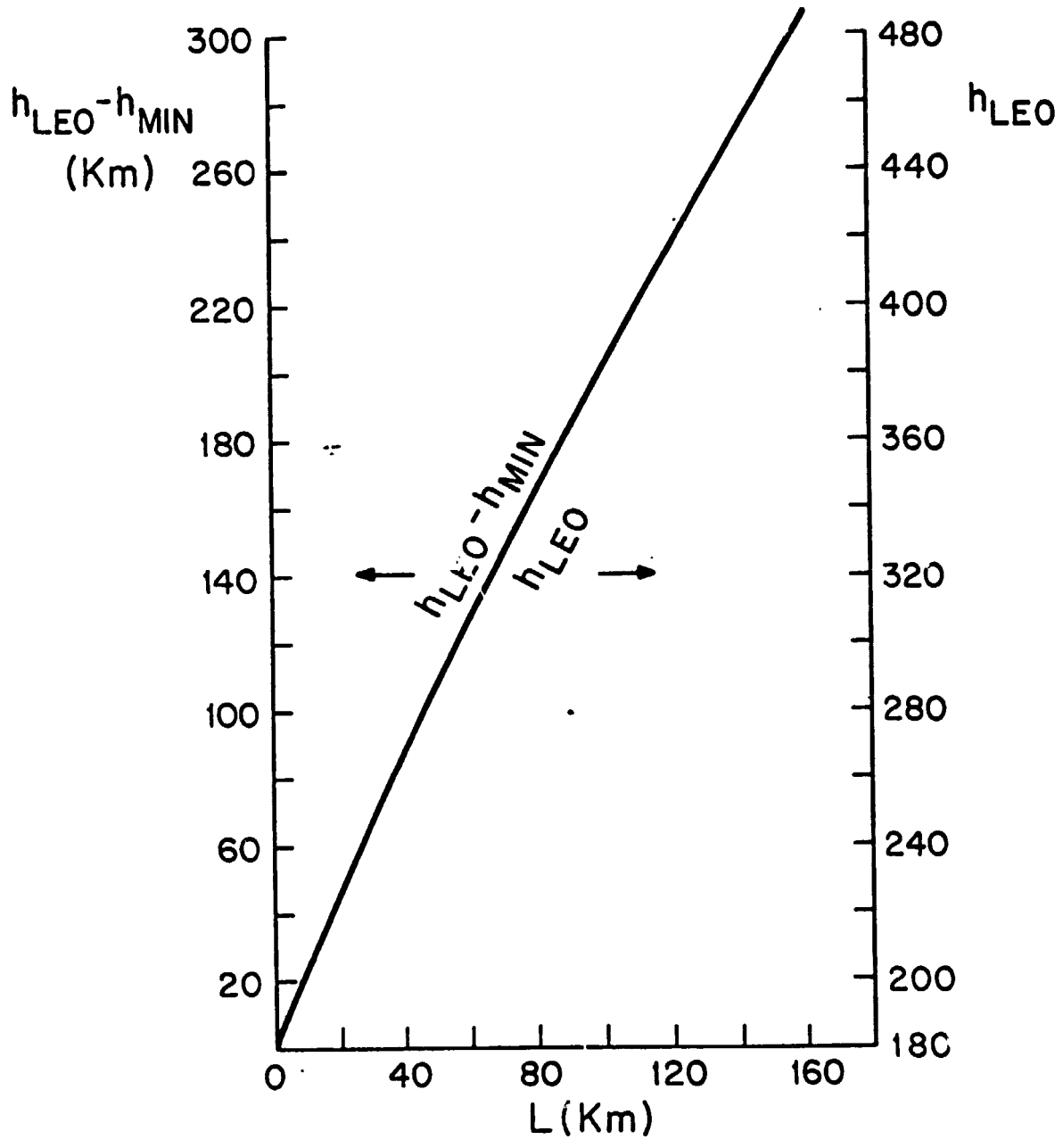

Fig. 2 Shuttle Altitude Loss (Left) and Tether Parking Altitude (Right), versus Tether Length (for case with maximum throw weight).

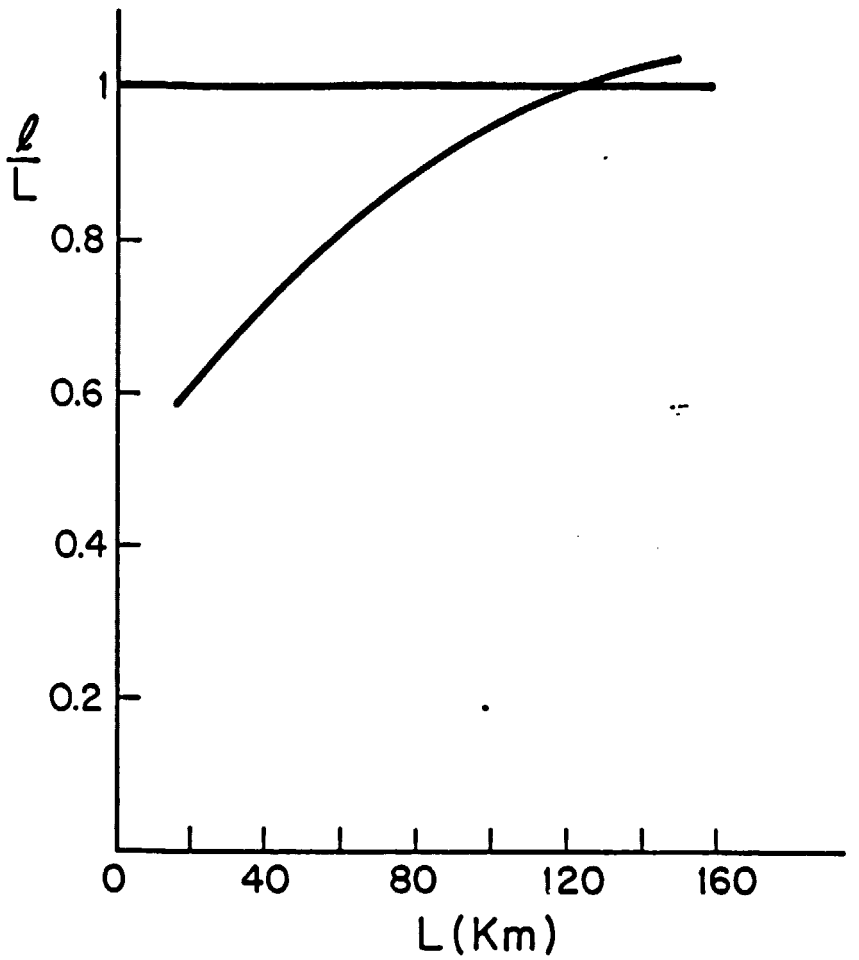

Fig. 3 Fraction of Tether Length Left Deployed at Shuttle Detachment (case with maximum throw weight).

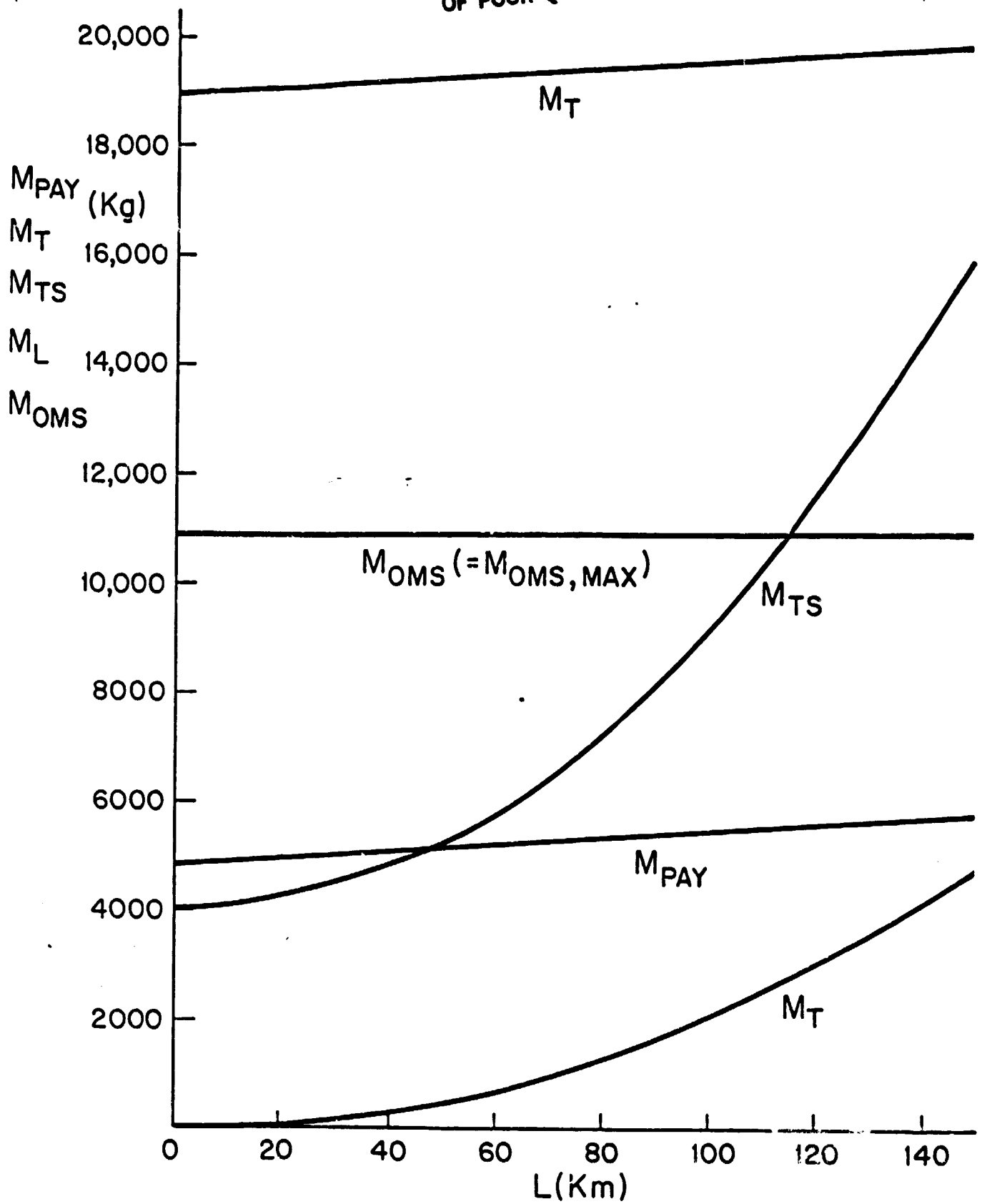

Fig. 4 Case with limited OMS fuel, fixed OTV vehicle variation of payload, loaded OTV mass and tether and tether system masses with tether length.

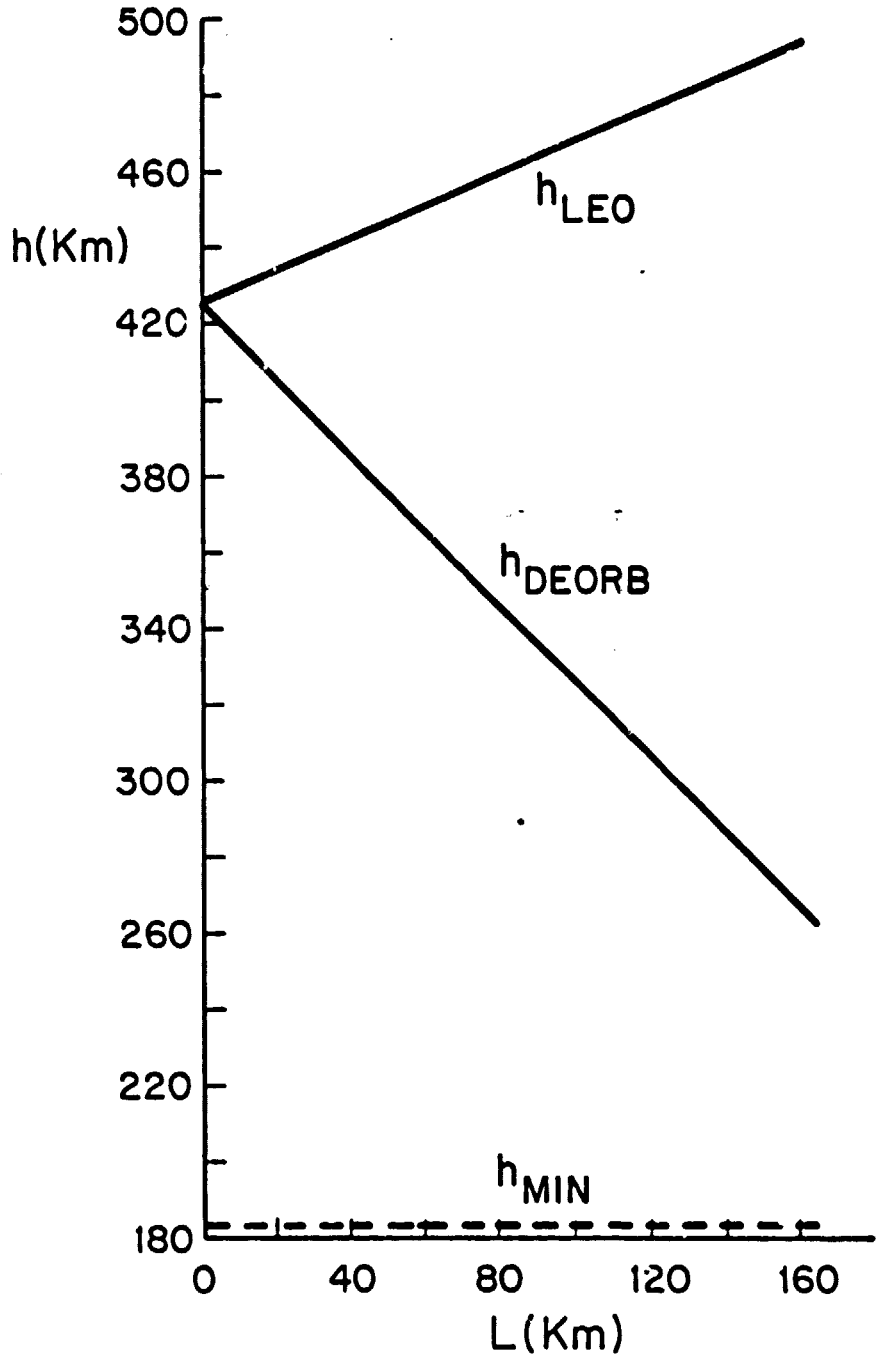

Fig. 5 Tether system parking altitude (h_{LEO}) and lowest shuttle altitude (h_{deorb}) versus tether length for case with fixed OTV, maximum OMS fuel also shown is minimum allowable altitude.

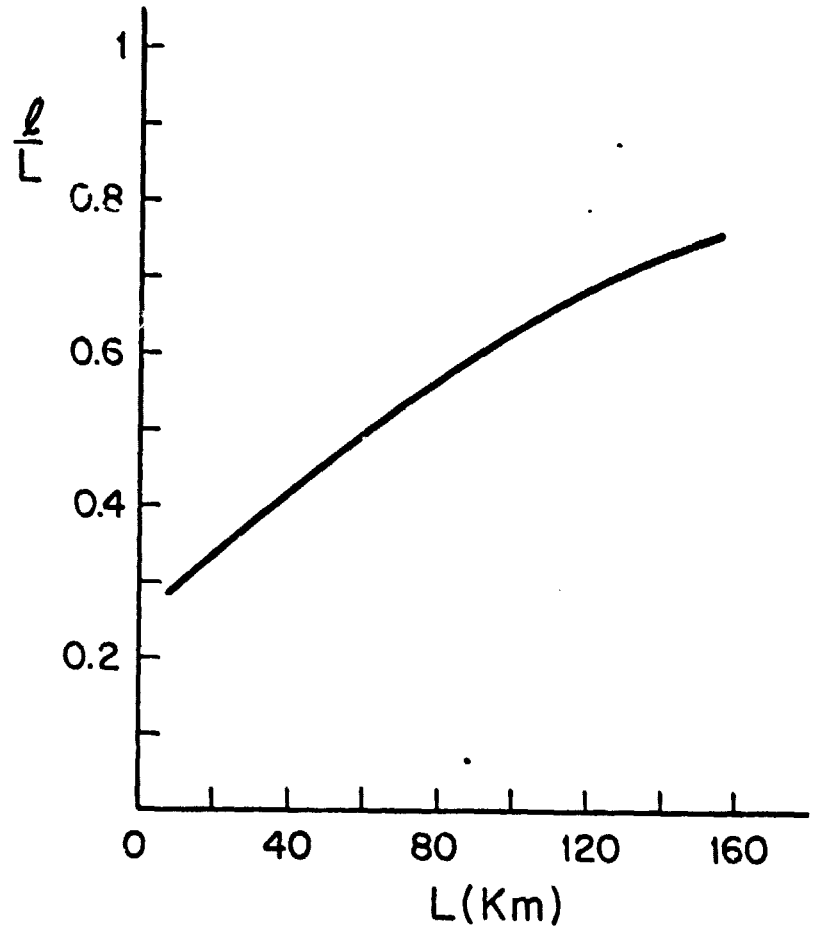

Fig. 6 Fraction of tether length left deployed at Shuttle detachment (case with fixed OTV and maximum OMS fuel).